Monitoring tau-tubulin interactions utilizing second harmonic generation in living neurons

William H. Stoothoff
Brian J. Bacskai
Bradley T. Hyman
Massachusetts General Hospital-Harvard Medical School
Department of Neurology
Charlestown, Massachusetts 02129

Abstract. Tau is a microtubule associated protein that is localized to the axon in neurons. During pathological conditions, including frontotemporal dementia (FTD), a shift in tau isoforms occurs that leads to enhanced expression of a form of tau with four (rather than three) microtubule binding repeats; this has been postulated to alter microtubule structure. Second harmonic generation (SHG) is a technique that allows the visualization of intact microtubules in axons of living neurons without the need for labeling or fixing. We examined how the presence of exogenous tau influences SHG in living neurons. Our results show that the presence of tau significantly enhances SHG, specifically in neuronal axons, despite the presence of tau throughout the entire cell. Our data also suggest that the presence or absence of the fourth microtubule binding repeat does not significantly alter tau's ability to enhance SHG. These results provide evidence that SHG is a useful, noninvasive tool to study tau-microtubule interactions in axons; further, it appears that tau overexpression, rather than specific isoforms, is the major contributor to tau-induced changes in axonal microtubule SHG signal.
[DOI: 10.1117/1.3050422]

Keywords: second harmonic generation; microtubule; Alzheimer's disease; tau protein; neuron; axon.

Paper 08055R received Feb. 15, 2008; revised manuscript received Sep. 4, 2008; accepted for publication Oct. 14, 2008; published online Dec. 30, 2008.

1 Introduction

Microtubules are dynamic, labile structures that undergo tight regulation by numerous proteins. Microtubules provide important functions for most cell types, including structural support, intracellular transport, and chromosome separation during cell division. Perhaps the most well-studied microtubule associated protein to date is tau protein, since changes in tau splicing and tau mutations lead to a neurodegenerative disease called frontotemporal dementia (FTD) with parkinsonism linked to chromosome 17 (FTDP-17), a clinical syndrome that leads to neuronal loss and dementia. Tau is also a key component of one of the pathological hallmarks of Alzheimer's disease (AD), the neurofibrillary tangle (NFT). Tau is uniquely localized in neurons and is associated with microtubules only in axons where the microtubules adopt an asymmetric conformation. Understanding the way in which tau and microtubules interact in living cells is crucial to understanding how disruption of this process might lead to cell dysfunction or death.

Approximately 50 tau gene mutations are associated with FTDP-17. Many of the mutations are within the introns adjacent to exon 10 and have been shown to alter tau splicing to favor inclusion of exon 10, which encodes an additional microtubule binding domain. Tau isoforms containing exon 10 are referred to as 4 repeat (4R) isoforms, whereas those lacking exon 10 are referred to as 3 repeat (3R) isoforms. Alterations of exon 10 splicing are also seen in nonfamilial cases of FTD,[1–8] supranuclear palsy,[8–10] and in some instances of AD.[3,8,11,12] We have also recently shown that alternative splicing of an amino terminal domain (exon 2) as well as exon 10 occur differentially in AD and control brain tissue.[12] Other FTDP-17 tau mutations lead instead to amino acid changes, often centered near the microtubule binding domains, and these are also believed to alter tau-microtubule dynamics. One of the most common of these mutations is the P301L mutation.[4,13–15]

These studies have provided valuable information about the marked effect tau splicing has in terms of association with neurodegeneration, but they have lacked a functional readout for the effect tau alterations have on intact microtubules within neurons. In isolated tau/tubulin preparations, the presence of the fourth microtubule binding repeat in tau appears to stabilize microtubules, unlike the isoforms that contain only three repeats.[16,17] By contrast, and somewhat contrary to expectations based on these *in vitro* data, recent fluorescence recovery after photobleaching (FRAP) data suggest that 3R tau and 4R tau have very similar properties with regard to tau/tubulin association in intact retinal ganglion cells.[18]

We have explored this issue using an alternative approach to examine the effect of tau splice forms on microctubules in intact neurons. Second harmonic generation (SHG) is a nonlinear optical microscopy method with inherent properties that

Address all correspondence to: Bradley T. Hyman, Massachusetts General Hospital, 114 16th Street, Charlestown, MA 02129. Tel: 617 726 2299; Fax 617 724 1480; E-mail: bhyman@partners.org.

1083-3668/2008/13(6)/064039/9/$25.00 © 2008 SPIE

make it suitable for visualizing microtubule structure in living cells. In SHG, light is generated by a structure at exactly one-half the wavelength of incident light; unlike fluorescence, the SHG signal can be elicited by a broad range of incident light, and the emitted photons "track" at exactly one-half the wavelength of incident light. Moreover, the process is nonabsorptive, so there is no photobleaching or free radical generation (for review, see Ref. 19). SHG arises only from inherently asymmetric chemical structures, including some biological molecules. A number of proteins have been shown to generate second harmonic signals, including collagen,[20,21] myosin,[22–24] and axonal microtubules,[19,25,26] with axonal microtubules being the weakest source of SHG.

In this study, we took advantage of the observation that axonal microtubules give rise to an SHG signal due to their asymmetric structure.[26] A disruption of axonal microtubules causes the loss of SHG signal.[26] We utilized SHG as a functional readout for microtubule structure in living cultured neurons and examined the effect of the presence of exogenous tau in transfected neurons. Our results clearly demonstrate that the presence of exogenous tau significantly enhanced SHG signal. Surprisingly, and in contrast to extrapolation from biophysical measures of isolated tau/microtubule interaction assays, our results suggest that the 3R and 4R isoforms of tau, and even a P310L FTDP-17-associated mutant form of tau, all seem to alter microtubules/SHG to a similar extent.

2 Experimental Procedures

2.1 *Cell Culture and Western Blot Analysis*

Primary cortical neurons were prepared from cerebral cortices of CD-1 strain mouse embryos (day 15 to 17 of gestation). Cortices were dissociated by trypsinization for 5 min at room temperature, and cells were resuspended in Neurobasal (NB) medium supplemented with 10% fetal bovineserum (FBS), 2 mmol/L glutamine (Gln), 100 U/ml penicillin, and 100 μg/ml streptomycin, then centrifuged at 100 g for 10 min and resuspended in NB/B27 [NB medium containing 2% (v/v) B-27 supplement], 100 U/ml penicillin, 100 μg/ml streptomycin, and 2 mmol/L Gln. The cells were then plated at 1×10^6 on 42-mm round coverslips (Hemogenix, Colorado Springs, CO), and coated with Poly-D-Lysine (20 μg/ml) in 60-mm cell culture dishes (Corning, Lowell, MA). Neurons were grown for 7 to 10 days *in vitro* and transiently transfected with the indicated constructs using Lipofectamine 2000 (Invitrogen, Carlsbad, CA) according to the manufacturer's protocol.

H4 human neuroglioma cells were maintained in Opti-MEM (Gibco, Carlsbad, CA) supplemented with 10% (v/v) FBS, 100 U/ml penicillin, and 100 μg/ml streptomycin (Gibco, Carlsbad, CA). Where indicated, cells were transiently transfected with the identified constructs using Lipofectamine 2000 (Invitrogen, Carlsbad, CA) according to the manufacturer's protocol.

Tau constructs were subcloned into either mRFP-N1 or eCFP-N1 vectors (Clontech, Mountainview, CA). Using Tau3R(−2−3), Tau3R(+2+3), Tau4R(−2−3), or Tau4R (+2+3) in pcDNA3.1(+) as templates, we performed polymerase chain reaction using the following primers: 5′-CTCGAGATGGCTGAGCCCCGCCAGGAGTTCGAAG-3′ (forward) and 5′-GGATCCAAACCCTGCTTGGCCAGGG AGGCAGAC-3′ (reverse), digested with Xho1 and BamH1 and ligated into appropriate color vectors. The integrity of each construct was verified using DNA sequencing analysis.

H4 human neuroglioma cells were transiently transfected with Lipofectamine 2000 according to the manufacturer's protocol and collected 48 hr post-transfection in 100-μl 2X sodium dodecyl sulfate (SDS) lysis buffer (0.25 M Tris-Cl, pH 7.5, 2% SDS, 5 mM ethylenediaminetetraacetic acid, 5 mM ethylene glycol tetraacetic acid, and 10% glycerol supplemented with a protease inhibitor pellet obtained from Gibco, Carlsbad, CA). Cell lysates were then sonicated for 10 sec and boiled for 10 min. Samples were centrifuged at room temperature for 10 min at 15,000 g. Sample concentrations were determined using the bicinchoninic acid assay (Pierce, Rockford, IL). Samples were diluted to 1 μg/μl in 2X SDS running buffer and loaded onto precast 4 to 12% Tris-Glycine gradient polyacrylamide gels (Invitrogen, Carlsbad, CA), electrophoresed, and transferred to polyvinylidene fluoride membranes. Membranes were blocked for 1 hr at room temp in Tris Buffered Saline Tween-20 (TBST) (20 mM Tris-Cl, pH 7.6, 137 mM NaCl, 0.05% Tween 20) and 5% milk and incubated in TBST and milk at 4 °C overnight in the indicated primary antibody. Membranes were then washed 3 times for 10 min in TBST at room temperature and incubated for 1 hr with appropriate horseradish peroxidase-conjugated secondary antibody in TBST and milk. Membranes were washed 3 times for 10 min in TBST at room temperature and visualized with enhanced chemiluminescence (Amersham, Piscataway, NJ).

2.2 *Live Cell Imaging and SHG*

Primary neurons on coverslips were fitted in a perfusion or culture (Hemogenix, Colorado Springs, CO) closed chamber with a 1-mm silicone gasket between glass coverslips. The chamber contained Hank's balanced salt solution (HBSS) prewarmed to 37 °C, and it was affixed in the heated stage of a Zeiss Axiovert 200 inverted microscope. All images were acquired on a Zeiss LSM-510 META confocal microscope fitted with a He/Ne 543-nm laser for red fluorescence protein (RFP) fluorescence and a Coherent (Santa Clara, CA) chameleon mode-locked Ti/Saph tunable (720 to 930 nm) laser with ~140-fs pulse width and ~20 to 30 mW average power with linear polarization at the sample, for cyan fluorescent protein (CFP) and SHG imaging. All images were acquired using a Zeiss 25×0.8 numerical aperture (NA) Plan-NEOFLUAR water/oil immersion lens for epifluorescence and an infinity-corrected Zeiss 20×0.75-NA PlanAPOCHROMAT dry lens affixed to a custom condenser tube (fabricated by Zeiss, Jana, Germany) affixed to the condenser housing, which projected the forward-propagating signal onto a photomultiplier tube (PMT, Hamamatsu). A 400 ± 25-nm bandpass filter was fitted between the condenser housing and the PMT. This aided in both reducing background fluorescence at the SHG PMT and in verifying the SHG nature of the signal observed, since 800-nm light was used to induce the SHG signal. The resulting 400-nm signal should pass through the filter unobstructed, while producing an SHG signal using 900 nm should result in a loss of the SHG signal, because the resulting 450-nm signal would be blocked by the bandpass

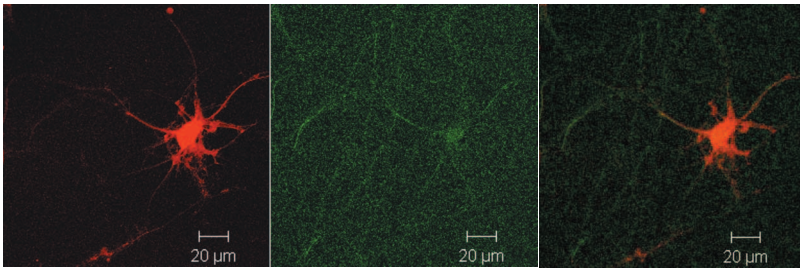

Fig. 1 Weak SHG signal is obtainable from nontransfected neurons. Photomicrograph showing a neuron transfected with RFP alone and visualized simultaneously in the 543/590-nm fluorescent excitation/emission signal (red) and 800/400-nm SHG excitation/emission (green). There is very little SHG present in cells that have endogenous levels of mouse tau expressed and that express RFP, but there is signal detectable. Micrograph represents of at least three neurons in each transfection from three separate mice.

filter. The bandpass filter also ensured that no fluorescent signal from the fluorophores would pass through to the PMT, since CFP emits around 450 nm and RFP emits around 590 nm, and both are blocked by the bandpass filter. To further ensure the signal obtained was from SHG and not autofluorescence, a polarizer was placed in front of the SHG PMT, and the polarizer was rotated to demonstrate the polarized nature of the SHG signal. Since the SHG signal is a polarized signal, rotating the polarizer perpendicular with respect to the laser polarization should result in a loss of SHG signal, in contrast to fluorescence emissions.

Images were collected using Zeiss LSM 3.5 software and exported as JPEG images for analysis in Image J. The Neuron J macro plugin for Image J was used to trace and quantify the SHG signal in all sample images, and the resulting intensity data were analyzed using Graphpad Prism 4 (San Diego, CA) to carry out t-tests or one-way analyses of variance (ANOVAs). Data were presented as mean $\pm$ SEM for each condition, and results were considered significant if $p < 0.05$.

3 Results

3.1 *Second Harmonic Generation Signal is Detectable in Single Neuronal Processes*

Recent work has shown that an SHG signal arises mainly from axonal processes in neurons, not from the cell body or dendrites,[26] in acute hippocampal slices. Therefore, we sought to determine whether it was possible to visualize an SHG signal from a single neuronal process in a cultured neuron that would allow us to visualize intact axonal microtubules in a living neuron. Figure 1 shows the morphology of a single neuron transfected with RFP and visualized with the red fluorescence signal. The RFP was excited with a 543-nm He/Ne laser, and the emitted light at 590 nm was directed to the PMT through a 570- to 610-nm bandpass filter. Similarly, the SHG signal was obtained with 800-nm excitation and collected in the forward direction after passing the signal through a 375- to 425-nm bandpass filter. A weak SHG signal was observed in single processes extending from each neuron. Several characteristics suggest that this was SHG: the 400-nm signal was seen only in the axon (as expected given the asymmetric microtubule structure unique to axons), whereas tau and autofluorescent moieties are most strongly seen in the cell body. This signal was lost when treated with colchicine, indicating that it was microtubule dependent. We inserted a polarizer in the light path between the sample and the PMT. Rotating the polarizer between 0 and 90 deg should either allow a polarized signal to pass or block a polarized signal, depending on the orientation, while fluorescent signals should be unaffected by the orientation of the polarizer. As expected, when the polarizer was in the 0-deg position, the SHG signal was strong. However, when the polarizer was shifted to the 90-deg position, the SHG signal was completely lost. As another test, we changed excitation wavelength to 900 nm, and the SHG signal observed in a 375 to 425 emission filter was lost, as would be expected for SHG (Fig. 2). Finally, we demonstrated that if the optics were reconfigured to detect the back-propagating signal, the signal was undetectable, again as expected for SHG—which is predominantly forward-propagating, unlike a fluorescent signal.

3.2 *Overexpression of Tau Increases the SHG Signal*

Next, we examined whether altering tau levels would enhance the SHG signal. As a first step, we characterized tau expression in H4 cells. Figure 3 shows a western blot analysis of various tau constructs expressed in H4 cells to verify the biochemical properties of each construct. The different isoforms' molecular weights corresponded to the presence or absence of the fourth microbutubule binding repeat (4R, representing exon 10) or the 2 amino-terminal inserts (+2+3). All constructs migrated to the expected molecular weight, indicating that the proteins were expressed and processed appropriately in cells.

We examined whether microtubules in H4 neuroglioma cells, which are morphologically flat with several long processes, would show SHG signal. No SHG signal could be detected from H4 cells transfected with CFP [Fig. 3(b)]. By contrast, imaging of H4 cells transfected with tau showed robust tau expression in the cell body and processes; interestingly, the SHG signal arose primarily from perinuclear compartments where tau levels were highest, and where the microtubule network appears to reorganize within the perikeria [Fig. 3(c)].

Next we examined whether transfection of tau would enhance SHG in neurons, and if so, in which cellular compartment. Given that tau is a microtubule binding protein that promotes the assembly and stability of microtubules in axons (reviewed in Ref. 27), it might follow that expression of tau would increase axonal SHG signal. To further test this hypothesis, and also to determine if the presence of a fluorescent

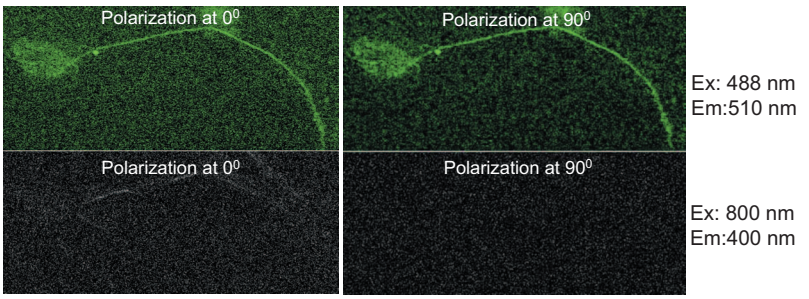

Fig. 2 SHG signal but not GFP signal is abolished by blocking polarized light with a polarizer. To conclusively demonstrate the SHG nature of the signal obtained in the SHG channel, a polarizer was placed in the light path of the SHG signal, and the orientation of the polarizer was positioned at either 0 or 90 deg. Both the GFP and SHG signals were obtained from GFPTau4R(+2+3)-transfected neurons. As expected, when the polarizer was changed and the GFP signal of tau-transfected neurons was obtained, there was no difference in the GFP signal. Conversely, the SHG signal was present only in the 0-deg position of the polarizer and was abolished when it was set to 90 deg, indicating the polarized nature of the SHG signal. This also rules out autofluorescent signals contaminating the SHG signal, because they would not be affected by the position of the polarizer. Micrograph represents of three neurons transfected with tau.

tag on tau would change the SHG, we transfected neurons with different isoforms of either TauRFP, untagged tau cotransfected with RFP, or RFP alone. SHG signal was measured by tracing SHG positive neurites using the Neuron J macro for Image J and analyzing the intensity across the entire length of the process.

Since transfection efficiency was very low in cultured neurons with our transfection method, it was possible to visualize the processes of a single neuron and follow them for many hundreds of microns without interference from the processes of neighboring, untransfected neurons. When TauRFP-transfected neurons were examined, the RFP fluorescence and SHG signals were distinct [Fig. 4(a)]: SHG signal was present in only one process, whereas the TauRFP fluorescence signal was present in multiple processes and the cell body. To verify that the signal obtained in the SHG channel was indeed SHG and not contaminating fluorescence, the wavelength of the

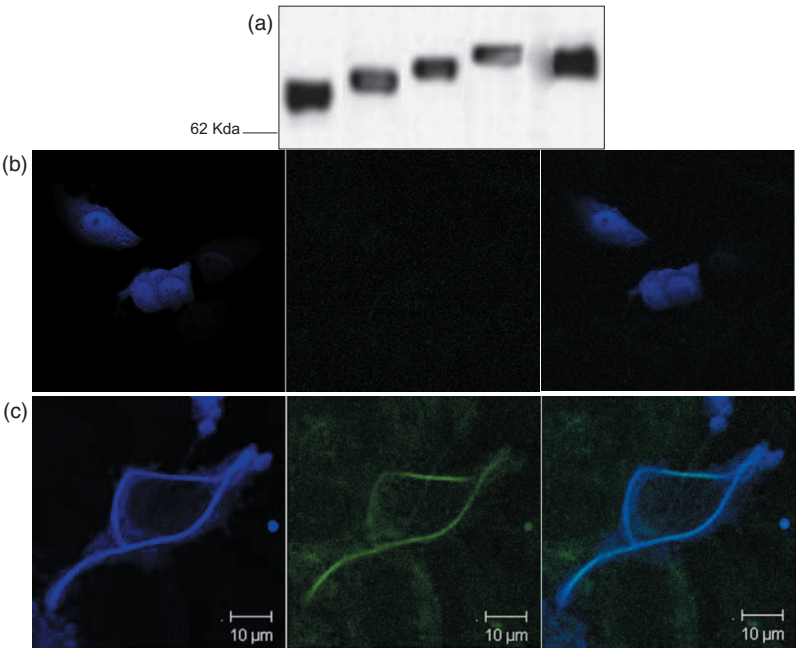

Fig. 3 Biochemical properties of tagged tau constructs are normal. Representative blot showing various tagged tau constructs that were transiently transfected into H4 human neuroglioma cells. (a) Cell lysates were immunoblotted and probed with a pan tau antibody (AB-3). Western blot shows that all expressed tau migrates to the expected molecular weight and that the presence of a C-terminal fluorescent protein (CFP or RFP) does not significantly alter tau processing. All constructs were transfected utilizing 1 μg of DNA per condition, and the total lysate protein concentration was normalized for each sample. (b) Expression of CFP in H4 neuroglioma cells leads to robust expression of CFP and fluorescence throughout the entire cell, with no SHG signal detectable in transfected cells. (c) Imaging of fluorescently tagged tau shows that tau is localized throughout the entire cell. SHG signal, however, comes from filamentous structures containing both tau and tubulin that encircle the nucleus and continue into the processes. Note specifically that the microtubule network seems to reorganize into circular structures in transfected H4 cells, and that robust SHG signal is present in more than one process. Photomicrographs are representative of at least three cells from each of at least three separate preparations.

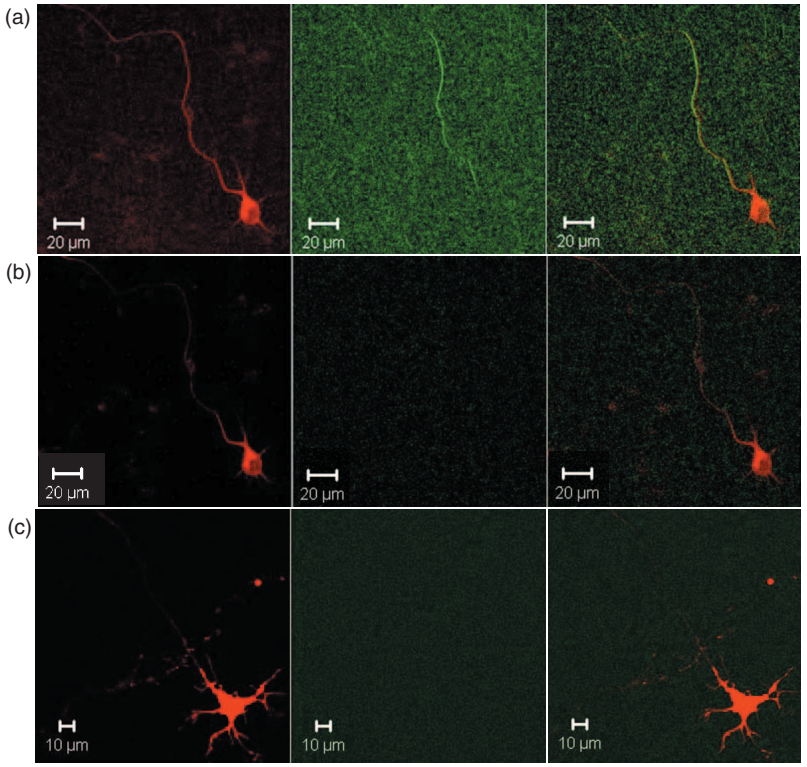

Fig. 4 Tau enhances SHG signal in transfected neurons. Embryonic day 15 mouse primary neurons were transfected with TauRFP for 48 hr, and individual transfected cells were examined for SHG signal. (a) Transfected neuron showing both TauRFP expression throughout neuron and SHG signal at 800 nm in a single process, which is presumably the axon. Final panel shows merged image. (b) Same cell as in (a) but showing TauRFP signal in the first panel and SHG signal when a 900-nm excitation wavelength is used in the second panel, thus demonstrating that SHG signal is not detectable when 900-nm excitation is used, as expected, because the bandpass filter before the SHG-detecting PMT cuts out all light above 425 nm. Third panel shows merged image. Micrographs are representative of at least three neurons per transfection from at least three separate mouse primary neuronal culture preparations. (c) Sister cultures of primary neurons as in (a) and (b) that were transfected with TauRFP and also treated with 100 μM colchicine for 30 min prior to imaging, which completely depolymerized the microtubules. First panel shows TauRFP signal in a cell and a similar amount of TauRFP expression as in (a) and (b). Second panel shows SHG signal, which is completely abolished as expected, indicating the microtubule nature of the SHG signal. Third panel shows merged image. Micrographs are representative of at least three transfected neurons for three separate mouse primary culture preparations.

excitation laser was changed from 800 nm to 900 nm. As expected, the SHG signal was abolished, since the bandpass filter in front of the SHG detector blocked 450-nm emission [Fig. 4(b)]. As a further control, we added a 450-nm bandpass filter to the turret, and we were able to switch between the 400-nm and 450-nm filters. Reconfiguring the detectors demonstrated that the signal was substantially forward-propagating and could not be detected in the back-propagating

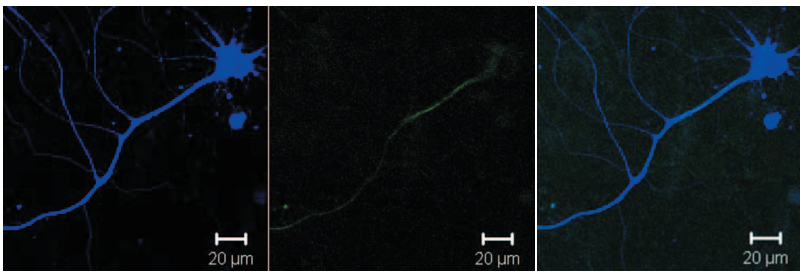

Fig. 5 Using circularly polarized light does not alter pattern of SHG in transfected neurons. Representative photomicrograph showing a single mouse neuron transfected with Tau4R(+2+3)CFP and visualized with 800-nm two-photon excitation. (a) TauCFP localization throughout the entire cell, including all processes and the cell body. (b) The forward-propagating SHG signal after circularly polarizing the excitation source, which should eliminate the dependence of the angle of orientation seen with linearly polarized light. Note that only a single process is still visible in the SHG channel, confirming that the primary neurite that is visible with SHG is the axon. (c) The merging of the first two images and co-localization of the SHG signal with tau in the axon, again indicating that TauCFP enhances SHG in only the axon. Micrographs are representative of at least three separate neurons from at least three separate transfections, all showing that circularly polarized light does not significantly affect the pattern of SHG signal.

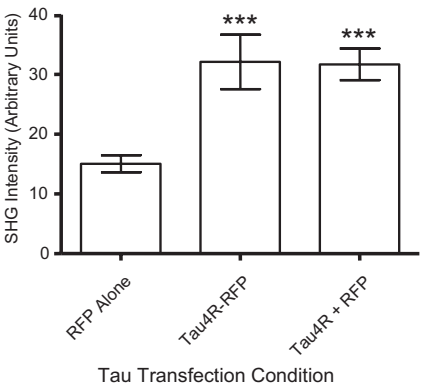

Fig. 6 Expression of either a tagged tau or untagged tau results in increased SHG. Mouse primary neurons were transiently transfected with either RFP alone, TauRFP, or Tau+RFP, and SHG signal was quantitated for each condition. The expression of RFP alone resulted in a modest amount of SHG signal (mean±SEM=15±1.5) while expression of either TauRFP (32.1±4.6) or Tau+RFP (31.7±2.6) resulted in a statistically significant increase in SHG signal; $p<0.001$ for each when compared to RFP alone ($n=15$ for each condition), $n=25$ neurons/condition. Interestingly, TauRFP and Tau+RFP were not significantly different.

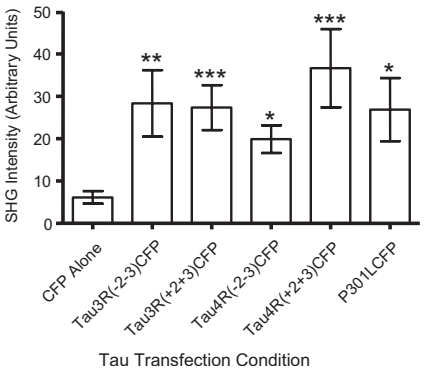

Fig. 7 Different tau isoforms do not significantly differ in their ability to enhance SHG. Primary mouse neurons were transiently transfected with the indicated tau isoform fused to CFP or CFP alone and SHG signal was measured. Note that CFP alone was different from all groups, and that there were no intergroup differences that were the result of tau isoform, or even the mutated P301L form of tau. CFP mean±SEM=6.12±1.48, Tau3R(−2−3)CFP=28.35±7.85, Tau3R(+2+3)CFP=27.34±5.31, Tau4R(−2−3)CFP=19.88±3.28, Tau4R(+2+3)CFP=36.65±9.26, TauP301L-CFP=26.85±7.45, and n=20 to 30 neurons per condition.

configuration (data not shown). As expected, when we used 800-nm light and the 400-nm filter, there was a detectable SHG signal. To test the hypothesis that the SHG signal observed was due to microtubule structures, sister cultures of TauRFP-transfected neurons were treated with 100-μM colchicine for 30 min and imaged as above. Since colchicine completely disrupts microtubule stability, any SHG signal arising from microtubules should be attenuated. As expected, treatment of cells with colchicine led to the complete loss of SHG signal [Fig. 4(c)]. These results clearly demonstrate that SHG signal is obtainable from a single neuronal process that is presumably the axon, and that the source of SHG signal within that process is the microtubule network.

As an additional control, we inserted a Berek compensator (New Focus, San Jose, CA) into the excitation light path (to circularly polarize the laser source) and examined the SHG signal from the processes. Figure 5 shows that, as expected, even when the excitation beam was circularly polarized, only one process showed a strong SHG signal.

Expression of either tagged or untagged tau led to a significant and equal increase in SHG signal (Fig. 6) over that of RFP alone (RFP=15.0±1.5, TauRFP=32.1±4.6, and Tau+RFP=31.7±2.6; $p<0.001$ for both RFP versus TauRFP and RFP versus Tau+RFP). The presence of either RFP or CFP fusion constructs on the C-terminus of tau did not further enhance or decrease the SHG signal from microtubules when compared to tranfection with untagged tau ($p>0.05$).

One possibility that could account for increased SHG signal from tau-transfected axons is that expression of tau significantly increases the overall diameter of the axon, and therefore increases the signal by giving rise to a signal from a larger axonal cross-section. To rule this out, images of axons of both RFP- or TauRFP-transfected neurons were examined in Image J, and the axonal diameter was measured at least 20-μm distal to the axon hillock and before the first major bifurcation of the axon. Three separate measurements per axon were averaged, and a two-tailed t-test revealed that there was no significant difference between RFP- and TauRFP-transfected axons. Therefore, tau expression does not increase SHG simply by increasing the size of the axon (data not shown).

3.3 *Different Tau Isoforms Do Not Significantly Differ in Enhancing SHG*

In *in vitro* assays, 4R tau binds microtubules with a greater affinity and polymerizes the formation of microtubules to a greater extent than 3R tau[16,28] (reviewed in Ref. 29). Having shown that tau enhances SHG signal in neurons, we next sought to determine whether different tau isoforms would differentially affect SHG signal. Tau-CFP constructs were generated for ease of planned co-transfection experiments, and in all instances they were equivalent to the transfection protocol utilized for the Tau-mRFP constructs used above. Neuronal cultures were transfected with one of the following constructs: CFP, Tau3R(−2−3)CFP, Tau3R(+2+3)CFP, Tau4R(−2−3)CFP, or Tau4R(+2+3)CFP. SHG signal was determined for each condition. As expected, the expression of any isoform of tau enhanced the observed SHG signal compared to empty-vector or CFP-transfected neurons (Fig. 7). Surprisingly, however, there was no significant difference between exon 10-containing or exon 10-skipping constructs, indicating that the presence of 3 or 4 microtubule binding repeats did not significantly affect tau's ability to enhance microtubule SHG signal in living neurons. No morphological changes in axon shape were noted qualitatively, and measuring the axon diameter revealed no difference between tau-transfected and control neurons.

Mutations in the tau gene found in FTDP-17 have been shown to decrease the *in vitro* association of tau with microtubules and the rate of microtubule polymerization.[13,17,30–34] To determine if tau mutations alter axon-derived SHG in living neurons, we transfected neurons with P301LTau4R(+2+3)CFP and examined the effect on SHG

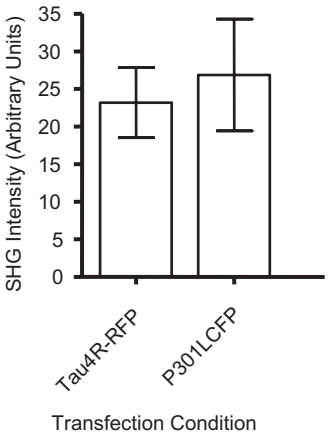

Fig. 8 FTDP-17 mutant tau does not differentially impact SHG generation.Primary mouse neurons were transiently transfected with indicated tau construct. Surprisingly, expression of either TauRFP or P301L-Tau4RCFP resulted in a high level of SHG signal with mean±SEM being 33.5±4.7 and 37.2±7.4, respectively, and n=20 to 30 neurons per condition.

signal. Surprisingly, the mutant tau enhanced the SHG signal observed in the transfected neurons (Fig. 8) to essentially the same extent as other tau isoforms.

4 Discussion

Our earlier studies suggested that axonal microtubule structures gave rise to SHG, as detected in bundles of axons in slice preparations,[26] and we proposed that the signal was due to a unique structure of axonal microtubules. Our current experiments demonstrate that the unique SHG signal can be detected in single axons. The signal is lost with the addition of the pharmacological disruption of microtubules by colchicine, and enhanced (only in axons) by transfection with the axonal microtubule binding protein tau, suggesting that tau-microtubule interactions gave rise to the enhanced signal. These data are consistent with the idea that the signal seen in axon bundles originates from the axonal microtubule structure itself rather than from extracellular compartments such as collagen or basement membrane. This observation further supports the idea that the source of SHG signal in axons is the asymmetric polarity of axonal microtubules.

Interestingly, H4 neuroglioma cells have very little or no SHG signal present, even in the many small neurites that encircle the cells. However, when tau is transfected into H4 cells, the microtubule network, along with tau, rearranges into circular filamentous structures that give rise to significant SHG signals. There are also multiple processes that can be observed with SHG signal-transfected H4 cells. These data suggest that H4 cells differ significantly from neurons in their processing of tau and the organization of microtubules within processes, and highlight the importance of studying tau-microtubule interactions in axonal compartments.

Our results, following tau transfections, were unexpected from several perspectives: overexpressed tau appeared in the soma and all processes of a neuron, and localized with tubulin in all cellular compartments. However, SHG signal was observed only in single processes. These data suggest that tau-tubulin interactions in the soma or dendritic processes do not stabilize microtubules into the same conformation in all cell compartments, and instead, that a unique conformation occurs in axons. The enhancement of SHG signal in these axonal compartments is consistent with the idea that excess tau (in the axon) can stabilize microtubules or enhance microtubule bundling; if so, these data using an *in vivo* biophysical measure in neocortical neurons complement and extend observations in retinal ganglion cells (RGCs) in which tau overexpression led to functional impairments in organelle transport.[33,35–39] Consistent with this idea, it was demonstrated by Mandelkow et al. that overexpressed tau leads to an increased density of microtubule bundles in axons,[40] and we postulate that this bundling underlies the enhanced SHG signal. Although it is not clear how this concept of being an improved SHG source compares to microtubule stability measured *in vitro*, our data demonstrate that overexpressed tau changes the biophysical properties of the axon in a striking fashion. One possibility that could account for increased SHG signal from tau-transfected axons is that expression of tau significantly increases the overall diameter of the axon, and therefore increases the signal from a larger axonal cross-section. To rule this out, images of axons of both RFP- or TauRFP-transfected neurons were examined in Image J, and the axonal diameter was measured at least 20-μm distal to the axon hillock and before the first major bifurcation of the axon. Three separate measurements per axon were averaged, and a two-tailed T-test revealed that there was no significant difference between RFP- and TauRFP-axons. Therefore, tau expression does not increase SHG by increasing the size of the axon (data not shown).

We hypothesized that 4R tau would enhance SHG to a greater extent than 3R tau. Our results suggest, however, that the presence of the fourth microtubule binding repeat had very little effect on microtubule SHG signal, implying that within the microenvironment of an intact axon, the presence of the fourth microtubule binding repeat does not significantly change the tau-induced microtubule conformation. This is consistent with the findings of Konzack et al., who demonstrated by using both FRAP and fluorescence correlation spectroscopy that the dwell time of a single molecule of tau on microtubules is very short, and that there was no significant difference between 3R and 4R tau with respect to how rapidly it diffused through the RGC axon or moved off and on the microtubules.[18] These data suggest that within the physiological environment of an axon, the tau isoform has little effect on microtubule-tau interactions.

The picture that emerges from our data is that tau interacts with microtubules in a specific asymmetric conformation in axons to generate a unique conformation that supports SHG. Using this assay of tau-microtubule interactions, it appears that the presence of the fourth microtubule binding repeat may exert less effect on the tau-microtubule interaction in axons than previously thought. Thus, although changes in tau splicing are clearly important in FTDP-17 and related conditions, our current data, as well as that of Konzack et al.,[18] suggest that the elevation of 4R tau may have additional pathogenic mechanisms independent of differential 3R versus 4R effects on axonal tau-microtubule interactions.

Acknowledgments

The authors would like to thank Dr. Jennifer M. Gass and Dr. Michael L. Hutton of the Mayo Clinic for their generous gifts of the Tau3R(−2−3), Tau3R(+2+3), Tau4R(−2−3), and Tau4R(+2+3) isoforms. We would also like to thank Brad Reynolds of Zeiss Microimaging for assistance with modifications of the LSM 510 instrumentation. This study was supported by National Institutes of Health AG 026249, EB000768, and P50 AG 05134.

References

1. A. Grover, H. Houlden, M. Baker, J. Adamson, J. Lewis, G. Prihar, S. Pickering-Brown, K. Duff, and M. Hutton, "5′ splice site mutations in tau associated with the inherited dementia FTDP-17 affect a stem-loop structure that regulates alternative splicing of exon 10," *J. Biol. Chem.* **274**(21), 15134–15143 (1999).
2. K. Ishizawa, H. Ksiezak-Reding, P. Davies, A. Delacourte, P. Tiseo, S. H. Yen, and D. W. Dickson, "A double-labeling immunohistochemical study of tau exon 10 in Alzheimer's disease, progressive supranuclear palsy and Pick's disease," *Acta Neuropathol. (Berl)* **100**(3), 235–244 (2000).
3. H. Ksiezak-Reding, B. Shafit-Zagardo, and S. H. Yen, "Differential expression of exons 10 and 11 in normal tau and tau associated with paired helical filaments," *J. Neurosci. Res.* **41**(5), 583–593 (1995).
4. M. G. Spillantini, R. A. Crowther, W. Kamphorst, P. Heutink, and J. C. van Swieten, "Tau pathology in two Dutch families with mutations in the microtubule-binding region of tau," *Am. J. Pathol.* **153**(5), 1359–1363 (1998).
5. M. G. Spillantini, J. R. Murrell, M. Goedert, M. R. Farlow, A. Klug, and B. Ghetti, "Mutation in the tau gene in familial multiple system tauopathy with presenile dementia," *Proc. Natl. Acad. Sci. U.S.A.* **95**(13), 7737–7741 (1998).
6. A. Delacourte, N. Sergeant, A. Wattez, D. Gauvreau, and Y. Robitaille, "Vulnerable neuronal subsets in Alzheimer's and Pick's disease are distinguished by their tau isoform distribution and phosphorylation," *Ann. Neurol.* **43**(2), 193–204 (1998).
7. N. Sergeant, J. P. David, D. Lefranc, P. Vermersch, A. Wattez, and A. Delacourte, "Different distribution of phosphorylated tau protein isoforms in Alzheimer's and Pick's diseases," *FEBS Lett.* **412**(3), 578–582 (1997).
8. M. Ingelsson, K. Ramasamy, C. Russ, S. H. Freeman, J. Orne, S. Raju, T. Matsui, J. H. Growdon, M. P. Frosch, B. Ghetti, R. H. Brown, M. C. Irizarry, and B. T. Hyman, "Increase in the relative expression of tau with four microtubule binding repeat regions in frontotemporal lobar degeneration and progressive supranuclear palsy brains," *Acta Neuropathol. (Berl)* **114**(5), 471–479 (2007).
9. N. Sergeant, A. Wattez, and A. Delacourte, "Neurofibrillary degeneration in progressive supranuclear palsy and corticobasal degeneration: tau pathologies with exclusively exon '10' isoforms," *J. Neurochem.* **72**(3), 1243–1249 (1999).
10. P. M. Stanford, G. M. Halliday, W. S. Brooks, J. B. Kwok, C. E. Storey, H. Creasey, J. G. Morris, M. J. Fulham, and P. R. Schofield, "Progressive supranuclear palsy pathology caused by a novel silent mutation in exon 10 of the tau gene: expansion of the disease phenotype caused by tau gene mutations," *Brain* **123**(Pt. 5), 880–893 (2000).
11. K. Yasojima, E. G. McGeer, and P. L. McGeer, "Tangled areas of Alzheimer brain have upregulated levels of exon 10 containing tau mRNA," *Brain Res.* **831**(1–2), 301–305 (1999).
12. C. Conrad, J. Zhu, C. Conrad, D. Schoenfeld, Z. Fang, M. Ingelsson, S. Stamm, G. Church, and B. T. Hyman, "Single molecule profiling of tau gene expression in Alzheimer's disease," *J. Neurochem.* **103**, 1228–1236 (2007).
13. E. W. Nagiec, K. E. Sampson, and I. Abraham, "Mutated tau binds less avidly to microtubules than wildtype tau in living cells," *J. Neurosci. Res.* **63**(3), 268–275 (2001).
14. D. Fischer, M. D. Mukrasch, M. von Bergen, A. Klos-Witkowska, J. Biernat, C. Griesinger, E. Mandelkow, and M. Zweckstetter, "Structural and microtubule binding properties of tau mutants of frontotemporal dementias," *Biochemistry* **46**(10), 2574–2582 (2007).
15. M. Hutton, C. L. Lendon, P. Rizzu, M. Baker, S. Froelich, H. Houlden, S. Pickering-Brown, S. Chakraverty, A. Isaacs, A. Grover, J. Hackett, J. Adamson, S. Lincoln, D. Dickson, P. Davies, R. C. Petersen, M. Stevens, E. de Graaff, E. Wauters, J. van Baren, M. Hillebrand, M. Joosse, J. M. Kwon, P. Nowotny, L. K. Che, J. Norton, J. C. Morris, L. A. Reed, J. Trojanowski, H. Basun, L. Lannfelt, M. Neystat, S. Fahn, F. Dark, T. Tannenberg, P. R. Dodd, N. Hayward, J. B. Kwok, P. R. Schofield, A. Andreadis, J. Snowden, D. Craufurd, D. Neary, F. Owen, B. A. Oostra, J. Hardy, A. Goate, J. van Swieten, D. Mann, T. Lynch, and P. Heutink, "Association of missense and 5′-splice-site mutations in tau with the inherited dementia FTDP-17," *Nature (London)* **393**(6686), 702–705 (1998).
16. M. Goedert, M. G. Spillantini, M. C. Potier, J. Ulrich, and R. A. Crowther, "Cloning and sequencing of the cDNA encoding an isoform of microtubule-associated protein tau containing four tandem repeats: differential expression of tau protein mRNAs in human brain," *EMBO J.* **8**(2), 393–399 (1989).
17. C. W. Scott, A. B. Klika, M. M. Lo, T. E. Norris, and C. B. Caputo, "Tau protein induces bundling of microtubules in vitro: comparison of different tau isoforms and a tau protein fragment," *J. Neurosci. Res.* **33**(1), 19–29 (1992).
18. S. Konzack, E. Thies, A. Marx, E. M. Mandelkow, and E. Mandelkow, "Swimming against the tide: mobility of the microtubule-associated protein tau in neurons," *J. Neurosci.* **27**(37), 9916–9927 (2007).
19. W. Mohler, A. C. Millard, and P. J. Campagnola, "Second harmonic generation imaging of endogenous structural proteins," *Methods* **29**(1), 97–109 (2003).
20. I. Freund, M. Deutsch, and A. Sprecher, "Connective tissue polarity. Optical second-harmonic microscopy, crossed-beam summation, and small-angle scattering in rat-tail tendon," *Biophys. J.* **50**(4), 693–712 (1986).
21. B. M. Kim, J. Eichler, K. M. Reiser, A. M. Rubenchik, and L. B. Da Silva, "Collagen structure and nonlinear susceptibility: effects of heat, glycation, and enzymatic cleavage on second harmonic signal intensity," *Lasers Surg. Med. Suppl.* **27**(4), 329–335 (2000).
22. M. Both, M. Vogel, O. Friedrich, F. von Wegner, T. Kunsting, R. H. Fink, and D. Uttenweiler, "Second harmonic imaging of intrinsic signals in muscle fibers in situ," *J. Biomed. Opt.* **9**(5), 882–892 (2004).
23. S. Plotnikov, V. Juneja, A. B. Isaacson, W. A. Mohler, and P. J. Campagnola, "Optical clearing for improved contrast in second harmonic generation imaging of skeletal muscle," *Biophys. J.* **90**(1), 328–339 (2006).
24. S. V. Plotnikov, A. C. Millard, P. J. Campagnola, and W. A. Mohler, "Characterization of the myosin-based source for second-harmonic generation from muscle sarcomeres," *Biophys. J.* **90**(2), 693–703 (2006).
25. D. Debarre, A. M. Pena, W. Supatto, T. Boulesteix, M. Strupler, M. P. Sauviat, J. L. Martin, M. C. Schanne-Klein, and E. Beaurepaire, "Second- and third-harmonic generation microscopies for the structural imaging of intact tissues," *Med. Sci. (Paris)* **22**(10), 845–850 (2006).
26. D. A. Dombeck, K. A. Kasischke, H. D. Vishwasrao, M. Ingelsson, B. T. Hyman, and W. W. Webb, "Uniform polarity microtubule assemblies imaged in native brain tissue by second-harmonic generation microscopy," *Proc. Natl. Acad. Sci. U.S.A.* **100**(12), 7081–7086 (2003).
27. W. H. Stoothoff and G. V. Johnson, "Tau phosphorylation: physiological and pathological consequences," *Biochim. Biophys. Acta* **1739**(2–3), 280–297 (2005).
28. R. Brandt and G. Lee, "Functional organization of microtubule-associated protein tau. Identification of regions which affect microtubule growth, nucleation, and bundle formation in vitro," *J. Biol. Chem.* **268**(5), 3414–3419 (1993).
29. M. Goedert, A. Klug, and R. A. Crowther, "Tau protein, the paired helical filament and Alzheimer's disease," *J. Alzheimers Dis.* **9**(3 Suppl.), 195–207 (2006).
30. J. H. Cho and G. V. Johnson, "Primed phosphorylation of tau at Thr231 by glycogen synthase kinase 3beta (GSK3beta) plays a critical role in regulating tau's ability to bind and stabilize microtubules," *J. Neurochem.* **88**(2), 349–358 (2004).
31. J. L. Ross, C. D. Santangelo, V. Makrides, and D. K. Fygenson, "Tau induces cooperative Taxol binding to microtubules," *Proc. Natl. Acad. Sci. U.S.A.* **101**(35), 12910–12915 (2004).
32. A. Samsonov, J. Z. Yu, M. Rasenick, and S. V. Popov, "Tau interaction with microtubules in vivo," *J. Cell. Sci.* **117**(Pt. 25), 6129–6141

(2004).
33. A. Seitz, H. Kojima, K. Oiwa, E. M. Mandelkow, Y. H. Song, and E. Mandelkow, "Single-molecule investigation of the interference between kinesin, tau and MAP2c," *EMBO J.* **21**(18), 4896–4905 (2002).
34. A. Sengupta, J. Kabat, M. Novak, Q. Wu, I. Grundke-Iqbal, and K. Iqbal, "Phosphorylation of tau at both Thr 231 and Ser 262 is required for maximal inhibition of its binding to microtubules," *Arch. Biochem. Biophys.* **357**(2), 299–309 (1998).
35. E. Thies and E. M. Mandelkow, "Missorting of tau in neurons causes degeneration of synapses that can be rescused by the kinase MARK2/Par-1," *J. Neurochem.* **27**(11), 2896–2907 (2007).
36. E. M. Mandelkow, K. Stamer, R. Vogel, E. Thies, and E. Mandelkow, "Clogging of axons by tau, inhibition of axonal traffic and starvation of synapses," *Neurobiol. Aging* **24**(8), 1079–1085 (2003).
37. K. Stamer, R. Vogel, E. Thies, E. Mandelkow, and E. M. Mandelkow, "Tau blocks traffic of organelles, neurofilaments, and APP vesicles in neurons and enhances oxidative stress," *J. Cell. Sci.* **156**(6), 1051–1063 (2002).
38. B. Trinczek, A. Ebneth, E. M. Mandelkow, and E. Mandelkow, "Tau regulates the attachment/detachment but not the speed of motors in microtubule-dependent transport of single vesicles and organelles," *J. Cell. Sci.* **112**(Pt. 14), 2355–2367 (1999).
39. A. Ebneth, R. Godemann, K. Stamer, S. Illenberger, B. Trinczek, and E. Mandelkow, "Overexpression of tau protein inhibits kinesin-dependent trafficking of vesicles, mitochondria, and endoplasmic reticulum: implications for Alzheimer's disease," *J. Cell. Sci.* **143**(3), 777–794 (1998).
40. E. M. Mandelkow, "The role of Tau in axonal transport and neurodegeneration," *Proc. ICAD 2008*, S02-03-06 (2008).